

# Advancements in Autonomous Mobility of Planetary Wheeled Mobile Robots: A Review

Mahboubeh Zarei<sup>1</sup> and Robin Chhabra<sup>1,\*</sup>

<sup>1</sup> *Mechanical and Aerospace Engineering, Carleton University, Ottawa, ON, Canada*

Correspondence\*:

Carleton University, 1125 Colonel by Drive, Ottawa, Ontario, K1S5B6  
robin.chhabra@carleton.ca

## 2 ABSTRACT

3 Mobility analysis is crucial to fast, safe, and autonomous operation of planetary Wheeled Mobile  
4 Robots (WMRs). This paper reviews implemented odometry techniques on currently designed  
5 planetary WMRs and surveys methods for improving their mobility and traversability. The methods  
6 are categorized based on the employed approaches ranging from signal-based and model-based  
7 estimation to terramechanics-based, machine learning, and global sensing techniques. They aim  
8 to detect vehicle motion parameters (kinematic states and forces/torques), terrain hazards (slip  
9 and sinkage) and terrain parameters (soil cohesion and friction). The limitations of these methods  
10 and recommendations for future missions are stated.

11 **Keywords:** Planetary Wheeled Mobile Robots, Odometry, Slip and Sinkage Estimation, Terrain Classification, Terramechanics

## 1 INTRODUCTION

12 For more than five decades, Wheeled Mobile Robots (WMRs) have been proven essential in space  
13 exploration and planetary missions. Traversing a wide range of environments, maneuverability, ability to  
14 be directed to special features, and lower weight and power consumption with respect to other platforms  
15 are some reasons supporting their increasing popularity. Figure 1 depicts the well-known WMRs in the  
16 past, present, and future missions on different extraterrestrial bodies. For a comprehensive bibliography  
17 on planetary WMRs the reader is referred to (Sanguino, 2017). The operation of WMRs on planetary  
18 bodies requires sophisticated software and hardware solutions for Guidance, Navigation and Control  
19 (GNC). This is indeed because of different conditions prevailed on extraterrestrial bodies. The complex  
20 and unknown environments, interaction with heterogeneous soil, steep slopes, loose and multi-phase  
21 terrains, driving over low gravity regions, harsh lighting conditions, unavailability of GPS signals, power  
22 consumption constraints, and computational limitations of embedded systems are critical challenges that  
23 must be dealt with when developing GNC modules (Quadrelli et al., 2015). Odometry or knowledge of pose  
24 and orientation of the vehicle with respect to some local references is a key component of GNC algorithms.  
25 Due to constraints and uncertainties involved, the current planetary WMRs rely on tele-communication with  
26 Earth-based stations to perform odometry and plan for safe operation. This ground-in-the-loop operation  
27 results in reduced time a vehicle can travel per day on a specific extraterrestrial body. As a result, future  
28 planetary missions demand for greater level of technology for localization to enhance the autonomy of  
29 roving platforms. In this paper, we first review the implemented odometry solutions on planetary WMRs  
30 and highlight their advantages and shortcomings. Then, we proceed with reviewing the solutions that  
31 have been proposed to improve the traversability and mobility of the planetary WMRs and aiding the

32 traditional odometry techniques. Here, we have categorized these solutions into five different approaches  
 33 including signal-based methods, model-based methods that rely on kinematics and estimation theory,  
 34 terramechanics-based methods, machine learning techniques, and global sensing.

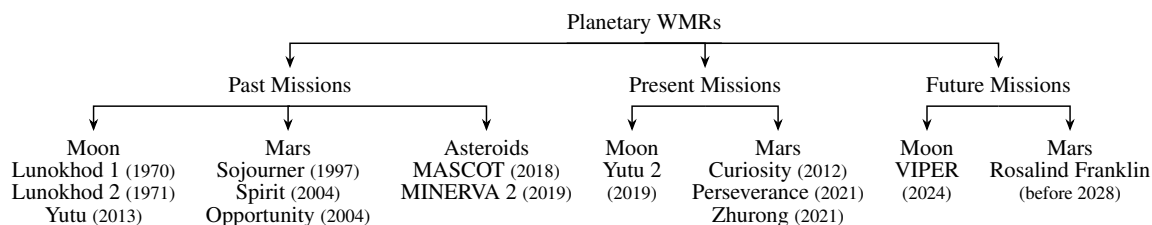


**Figure 1.** Planetary WMR platforms, date, and site of missions

## 2 IMPLEMENTED NAVIGATION TECHNIQUES ON PLANETARY WMRs

35 Odometry is central to every navigation system. It refers to estimating pose and orientation of a vehicle  
 36 with respect to some reference coordinate frames. Odometry can be performed using proprioceptive sensing  
 37 (e.g. IMU and encoders) or exteroceptive sensing (e.g. camera and Sun sensor). Therefore, depending  
 38 on the sensors involved the problem is called Wheel Odometry (WO), Inertial Odometry (IO), or Visual  
 39 Odometry (VO). The WO uses a kinematic model of the vehicle along with the rotational velocity of  
 40 the wheels, acquired by the encoders, to estimate pose and orientation. The drift of this method on even  
 41 and planar terrains is above 10% of the traversed distance (Azkarate Vecilla, 2022). This solution was  
 42 implemented on Sojourner in Mars Pathfinder mission in 1997 for pose estimation (Matijevic, 1997b).  
 43 Other Mars rovers of Jet Propulsion Laboratory (JPL) use this type of odometry in combination with other  
 44 means. The IO uses noisy measurements of inertial sensors and a kinematic model to estimate pose and  
 45 orientation. The noise level of accelerometers results in 5-10% drifts in estimating pose making the IO  
 46 ineffective in translational motion. However, it has been used to accurately update the rotational states.  
 47 Using sensor fusion through Kalman-based filters combined WO and IO was proposed in (Baumgartner  
 48 et al., 2001; Ali et al., 2005) to ensure the accurate odometry on high-traction terrains for Spirit and  
 49 Opportunity rovers of Mars Exploration Rover (MER) missions. This technique was also aided by a Sun  
 50 sensor to provide absolute heading estimations. The VO processes a sequence of onboard camera images  
 51 for motion estimation. This method is independent of wheel-terrain interactions and provides accurate  
 52 estimates (1-5% drifts). The rover Curiosity of Mars Science Laboratory (MSL) mission and Perseverance  
 53 rover of Mars2020 mission combine the previously stated odometry methods with VO (Gong, 2015). The  
 54 Rosalind Franklin rover of ExoMars mission employs combined VO and IO for its localization (Bora  
 55 et al., 2017). The VO was also implemented on the Lunar rover Yutu 2 of Chang'e 4 mission (Wan et al.,  
 56 2014). The combined WO, IO, and VO can produce estimates with 1-2% of drift (Azkarate Vecilla, 2022).  
 57 Although VO provides a superior performance for localization, it is computationally expensive which  
 58 negatively affects power consumption and speed of a WMR. To resolve this problem Field-Programmable  
 59 Gate Arrays (FPGAs) was proposed as an efficient platform for running VO (Howard et al., 2012). Table 1  
 60 summarizes the odometry techniques for planetary WMRs and compares their performance.

**Table 1.** Comparison of different odometry methods for planetary WMRs.

Method	Accuracy (% traversed distance )	Frequency (Hz)	Advantages	Limitations
WO	10	10-100	-simple structure -not computationally demanding	-high drifts for uneven and deformable terrains
IO	5-10	10-100	-self contained -not computationally demanding	-error accumulation of accelerometers
VO	1-5	0.5	-immune to error accumulation -independent of terrain	-computationally demanding -low-speed operation
Combined	1-2	10	-enhanced accuracy	-complex structure -low-speed operation

### 3 MOBILITY AND TRAVERSABILITY ENHANCEMENT

61 To increase the operation time, future planetary WMRs require a higher degree of autonomy to perform  
 62 navigation tasks without relying on high-latency tele-communication with Earth-based stations. However,  
 63 operation on extraterrestrial bodies is not analogous to Earth operations and involves challenging problems.  
 64 For instance, driving on soft deformable and non-homogeneous soil, steep slopes, few distinguishable  
 65 visual features, permanent shaded areas, and processing power constraints on embedded systems are some  
 66 of these challenges. These problems demand for design of specific algorithms that are capable of predicting  
 67 traversability for planning safe autonomous operations and improving mobility and odometry on unknown  
 68 rough terrains. This section surveys dozens of these methodologies.

#### 69 3.1 Direct Signal-based Approaches

70 These approaches use output signals of some sensors to detect abnormal conditions and correct odometry.  
 71 Hardware redundancy, use of special sensors, frequency analysis, and logic reasoning are some methods in  
 72 this category. Fuzzy logic and expert rule-based techniques were used in (Ojeda et al., 2004) to compare  
 73 data from redundant encoders with each other, gyros, and motor currents to detect slip and correct odometry  
 74 for a six-wheel robot with a rocker-boogie suspension system. However, this technique does not estimate  
 75 the degree of wheel slip. (Ojeda et al., 2006) proposed a slip estimator for odometry correction in the  
 76 direction of motion that requires accurate current measurements and some specific terrain parameters.  
 77 They argue that the terrain parameters can be estimated online either using absolute positions provided by  
 78 GPS or induced slip in a single wheel for a WMR with at least four driven wheels. The slip detection in  
 79 Mars rover Curiosity, is done based on motor currents and visual sensors (Arvidson et al., 2017). When  
 80 abnormal currents are detected the vision system is activated to aid the navigation system with VO. In case  
 81 features are not unique in the scene, using wheel tracks (Maimone et al., 2007) or steering mast cameras  
 82 are proposed (Strader et al., 2020). Visual odometry correction on deformable terrains were also proposed  
 83 in (Reina et al., 2010) using fuzzy reasoning and in (Nagatani et al., 2010) using special telecentric lens.  
 84 These techniques, however, require high computational cost on embedded processors of planetary WMRs.  
 85 Thermal cameras are another form of special sensors that were used in (Cunningham et al., 2015) to develop  
 86 a non-geometrical method for predicting traversability of a terrain through analysing its thermal inertia  
 87 from infrared imagery. However, long observation periods are required to obtain a good prediction.

#### 88 3.2 Estimation and Kinematics

89 These methods are based on kinematics models derived from the physics of WMRs and estimation theory  
 90 tools such as Kalman-based filters. In (Dissanayake et al., 2001), nonholonomic kinematic constraints  
 91 were used to obtain velocity measurements for aiding the IO within an Extended Kalman Filter (EKF)

92 framework. The method, however, is not applicable on low-traction and uneven terrains of extraterrestrial  
93 bodies as the authors modeled slip as a zero-mean noise. Other kinematics-based methods that aim to  
94 improve odometry performance were proposed in (Hidalgo-Carrío et al., 2014; Lou et al., 2019). A vision-  
95 based method was proposed in (Helmick et al., 2006) which developed a forward kinematics model of  
96 rocker–bogie suspension system for a Kalman filter to combine inertial and visual measurements as well as  
97 wheel rates and wheel steering angles for slip estimation and compensation. However, permanent shaded  
98 regions of Moon, featureless scenes of Mars, and power constrains of WMRs are the main limitations  
99 of visual techniques. In (Ward and Iagnemma, 2008) a tire traction model within an EKF framework  
100 was incorporated to fuse data of encoders, IMU, and GPS for detecting slip and immobilized conditions.  
101 However, GPS signals are not available on extraterrestrial bodies. Although, most research works rely on  
102 EKF for estimation, in (Sakai et al., 2009; Reina et al., 2020) two different filters were used. The former  
103 proposed a 6-DoF localization solution within an Unscented Kalman Filter (UKF) framework based on the  
104 measurements of stereo cameras, an IMU, and wheel encoders. The latter employed a Cubature Kalman  
105 Filter (CKF) to estimate terrain properties using vibrations. To reduce odometry error of combined IO and  
106 WO, (Kilic et al., 2019) employed nonholonomic constraints and the zero-velocity updates with periodic  
107 stops. The autonomous stopping times through estimating and monitoring wheel slip were investigated  
108 in (Kilic et al., 2021). However, these methods sacrifice accuracy for traverse rate. In (Malinowski et al.,  
109 2022) the effect of integration of predicted slip in WO and VO was investigated using an EKF architecture.

### 110 3.3 Terramechanics and Dynamics

111 Terramechanics studies soil properties and wheel-terrain interactions to find normal and shear stresses  
112 developed at the contact areas using, e.g., empirical Bekker-Wong models (Bekker, 1969; Wong and  
113 Reece, 1967) and their recent modification (Higa et al., 2015). The Mars rover Sojourner performed  
114 parameter estimation of Martian soil to identify cohesion and internal friction angle relying on Earth-based  
115 analyses (Matijevic, 1997a). However, Earth-in-the-loop procedures are time consuming and inefficient.  
116 Online estimation of these parameters were proposed in (Iagnemma et al., 2004) based on simplified  
117 terramechanic equations and a least squares technique that identifies the parameters using measurements of  
118 the rover configuration sensors, encoders, potentiometers, and six-axis force/torque sensors. The simplified  
119 terramechanics-based models were also used in (Ishigami et al., 2007) to deal with longitudinal and  
120 lateral slip during steering manoeuvres on deformable soil. However, the accuracy of the estimations is  
121 under doubt, since simplified models are not a good representation of real interactions. In (Higa et al.,  
122 2016), six-axis force/torque sensors and five types of custom-built contact sensors were used to obtain  
123 the three-dimensional stress distribution at the wheel-terrain contact area on lunar regolith simulant. The  
124 method, however, for a single wheel results in an error of 1-11%. Real-time estimation of terrain parameters  
125 was also addressed in (Li et al., 2018) using semi-empirical terramechanic equations and EKF for WMRs  
126 driving on deformable slopes. However, this method is not useful for untraversed areas as it requires a  
127 history of measurement data. To measure the terramechanic parameters ahead of the rover, (Zhang et al.,  
128 2022b) proposed use of an articulated wheeled bevameter equipped with force and vision sensors to predict  
129 the slip and sinkage of wheels. An in-situ method for estimating sinkage was given in (Guo et al., 2020)  
130 that defines a new reference line of wheel sinkage and simplifies terramechanics into closed-form equations  
131 using force/torque sensors. The method is limited to moderate and high-traction terrains.

### 132 3.4 Machine Learning Approaches

133 These approaches are mainly based on classification or regression techniques to respectively provide  
134 discrete or continuous estimates of the quantities of interest. A terrain classifier was trained using vibration

135 signals measured by an accelerometer, which is subject to noise and bias (Brooks and Iagnemma, 2005). The  
136 training process was also offline making the method inappropriate for unknown environments. To alleviate  
137 its shortcomings, the same authors proposed a self-supervised learning method that predicts the terrain  
138 properties using two distinct classifiers (Brooks and Iagnemma, 2012). The Support Vector Machine (SVM)  
139 proprioceptive classifier analyzes vibration signals or combination of torques and sinkage to generate  
140 labels for training an exteroceptive terrain classifier. The second SVM classifier uses stereo imagery to  
141 identify potentially hazardous terrains from a distance. However, this training method is uni-directional  
142 where vibration signals are only used to train the visual classifier. To improve the training procedure, (Otsu  
143 et al., 2016) proposed a bi-directional training technique where the two classifiers train each other. In  
144 the context of slip estimation, Omura and Ishigami (2017) proposed a SVM learning technique based on  
145 the measurements of the normal force and contact angle at the wheel-terrain interaction area to generate  
146 correlation labels for the slip and classify wheel slip into three levels: non-stuck, quasi-stuck, and stuck.  
147 (Gonzalez et al., 2018a) compared the performance of supervised (artificial neural networks and SVM) and  
148 unsupervised (self organizing map and k-means) classification techniques in detection of three discrete  
149 levels for longitudinal slip (low, moderate, and high) based on the measurements of IMU, encoders, and  
150 motor currents. A vision-based classification method was proposed in Endo et al. (2021) to predict wheel  
151 slip via estimating terrain slopes. The computational cost of image processing limits the use of visual  
152 approaches. Deep learning techniques were also proposed for proprioceptive terrain classification based  
153 on the measurements of motion states and wheel forces/torques (Vulpi et al., 2020). At best its error is  
154 around 8.6%. The main limitation of these methods is that slip cannot be estimated in a continuous manner  
155 and the outputs are only useful to avoid hazardous terrains. In (Angelova et al., 2007), continuous slip  
156 was predicted from a distance based on visual data and nonlinear regression models that correlates terrain  
157 appearance and geometry with slip. The applicability of the method is under doubt since, it uses visual  
158 sensors and it has some difficulties to determine the terrain types. In (Gonzalez et al., 2018b) Gaussian  
159 Process Regression (GPR) is used to predict continuous slip and its variance based on the measurements of  
160 IMU and motor torques. However, the computational effort of GPR is high as it uses the history of features  
161 to perform its predictions. The GPR was also employed on China's Mars rover Zhurong to estimate the  
162 average of longitudinal and lateral slip using the measurements of IMU, encoders, and motor currents  
163 (Zhang et al., 2022a).

### 164 **3.5 Global Sensing**

165 Global localization solutions are incorporated to bypass limitations of the odometry and correct its  
166 position drifts. A tele-communication link between Mars orbiter Odyssey and MER platforms enabled the  
167 navigation system to obtain position accuracy of about 10 meters around three days (Guinn, 2001). Skyline  
168 signature matching between images captured by a WMR and a global map was proposed in (Chiodini  
169 et al., 2017) to initialize the vehicle position after landing on Mars. (Matthies et al., 2022) proposed an  
170 onboard global localization technique which involves mapping Lunar craters from orbit and then using  
171 stereo cameras or LiDAR for detecting the craters landmarks. The accuracy of this method depends on  
172 the resolution of global maps. Learning algorithms such as Siamese Neural Networks were proposed for  
173 global localization on Mars and moon respectively in (i Caireta, 2021) and (Wu et al., 2019).

### 174 **3.6 Summary and Potential Future Directions**

175 Table 2 summarizes the methodologies discussed throughout this section and indicates their potential  
176 applications for improving mobility and traversability of planetary WMRs. The level of feasibility of  
177 these solutions leaves plenty of room for improvement. One major problem is computational limitations

178 of embedded systems within these robots, and future research must be directed toward developing  
 179 computationally efficient software solutions on available hardware. Distributed sensing, either sensor-level  
 180 or track-level fusion, can be used in the estimation architecture to enhance its performance. To achieve  
 181 greater level of autonomy, the prospective learning solutions should be designed based on multi-directional  
 182 communicating training techniques. Novel terramechanics models based on updated information on  
 183 planetary surfaces (e.g., soil composition, surface geometry) are needed to simultaneously enhance fidelity  
 184 and efficiency of the traditional models. Fast and robust vision-based algorithms must be developed to  
 185 detect and match features in harsh lighting conditions and featureless environments of extraterrestrial  
 186 bodies. Another prospective solution is combining different approaches, reviewed in this section, to design  
 187 robust systems for high-speed navigation of future planetary WMRs.

**Table 2.** Summary of mobility and traversability enhancement methodologies for planetary WMRs.

Approach	Potential Applications	Advantages	Disadvantages
Direct signal-based	-hazard avoidance -slip estimation -odometry correction	-simple structure	-extra hardware cost -requiring accurate measurements -no single systematic approach
Estimation and kinematics	-odometry correction -slip estimation -immobilization detection -terrain properties estimation -soil properties estimation	-well-studied tools -systematic solutions -improved reliability using sensor fusion	-errors in system and noise models
Terramechanics and dynamics	-slip estimation -stress estimation -sinkage estimation	-applicable on deformable and uneven terrains	-modeling errors -requiring special hardware -wheel-level tests
Machine learning	-hazard avoidance -slip estimation -terrain properties estimation	-improved autonomy	-computationally demanding -depending on training process -vulnerable to noise
Global sensing	-odometry correction -hazard avoidance	-improved accuracy	-computationally demanding -depending on resolution of global maps

## 4 CONCLUSIONS

188 This paper surveyed dozens of methodologies for mobility analysis and mission planing of planetary  
 189 WMRs. The performance of the currently implemented odometry methods was compared and potential  
 190 solutions for improvement of these methods were discussed. Further research is still demanded to improve  
 191 the practicality and performance of the proposed methods. Future research should be directed toward  
 192 reducing computational burdens on embedded systems, use of distributed estimation and multi-directional  
 193 learning techniques, developing terramechanics models for planetary interfaces, and designing fast and  
 194 robust vision-based algorithms for high-speed operation of planetary WMRs.

## REFERENCES

- 195 Ali, K. S., Vanelli, C. A., Biesiadecki, J. J., Maimone, M. W., Cheng, Y., San Martin, A. M., et al. (2005).  
 196 Attitude and position estimation on the mars exploration rovers. In *2005 IEEE International Conference*  
 197 *on Systems, Man and Cybernetics* (IEEE), vol. 1, 20–27

- 198 Angelova, A., Matthies, L., Helmick, D., and Perona, P. (2007). Learning and prediction of slip from visual  
199 information. *Journal of Field Robotics* 24, 205–231
- 200 Arvidson, R. E., Iagnemma, K. D., Maimone, M., Fraeman, A. A., Zhou, F., Heverly, M. C., et al. (2017).  
201 Mars science laboratory curiosity rover megaripple crossings up to sol 710 in gale crater. *Journal of*  
202 *Field Robotics* 34, 495–518
- 203 Azkarate Vecilla, M. (2022). *Autonomous navigation of planetary rovers*. Ph.D. thesis, University of  
204 Malaga
- 205 Baumgartner, E. T., Aghazarian, H., and Trebi-Ollennu, A. (2001). Rover localization results for the fido  
206 rover. In *Sensor Fusion and Decentralized Control in Robotic Systems IV* (Spie), vol. 4571, 34–44
- 207 Bekker, M. G. (1969). *Introduction to terrain-vehicle systems. part i: The terrain. part ii: The vehicle*.  
208 Tech. rep., Michigan Univ Ann Arbor
- 209 Bora, L., Nye, B., Lancaster, R., Barclay, C., and Winter, M. (2017). Exomars rover control, localisation  
210 and path planning in an hazardous and high disturbance environment. In *14th Symposium on Advanced*  
211 *Space Technologies in Robotics and Automation (ASTRA)*. 20–22
- 212 Brooks, C. A. and Iagnemma, K. (2005). Vibration-based terrain classification for planetary exploration  
213 rovers. *IEEE Transactions on Robotics* 21, 1185–1191
- 214 Brooks, C. A. and Iagnemma, K. (2012). Self-supervised terrain classification for planetary surface  
215 exploration rovers. *Journal of Field Robotics* 29, 445–468
- 216 Chiodini, S., Pertile, M., Debei, S., Bramante, L., Ferrentino, E., Villa, A. G., et al. (2017). Mars rovers  
217 localization by matching local horizon to surface digital elevation models. In *2017 IEEE International*  
218 *Workshop on Metrology for AeroSpace (MetroAeroSpace)* (IEEE), 374–379
- 219 Cunningham, C., Nesnas, I., and Whittaker, W. L. (2015). Terrain traversability prediction by imaging  
220 thermal transients. In *2015 IEEE International Conference on Robotics and Automation (ICRA)* (IEEE),  
221 3947–3952
- 222 Dissanayake, G., Sukkarieh, S., Nebot, E., and Durrant-Whyte, H. (2001). The aiding of a low-cost  
223 strapdown inertial measurement unit using vehicle model constraints for land vehicle applications. *IEEE*  
224 *transactions on robotics and automation* 17, 731–747
- 225 Endo, M., Endo, S., Nagaoka, K., and Yoshida, K. (2021). Terrain-dependent slip risk prediction for  
226 planetary exploration rovers. *Robotica* 39, 1883–1896
- 227 Gong, W. (2015). Discussions on localization capabilities of msl and mer rovers. *Annals of GIS* 21, 69–79
- 228 Gonzalez, R., Apostolopoulos, D., and Iagnemma, K. (2018a). Slippage and immobilization detection for  
229 planetary exploration rovers via machine learning and proprioceptive sensing. *Journal of Field Robotics*  
230 35, 231–247
- 231 Gonzalez, R., Fiacchini, M., and Iagnemma, K. (2018b). Slippage prediction for off-road mobile robots via  
232 machine learning regression and proprioceptive sensing. *Robotics and Autonomous Systems* 105, 85–93
- 233 Guinn, J. R. (2001). Mars surface asset positioning using in-situ radio tracking. In *Proceedings AAS/AIAA*  
234 *Space Flight Mechanics Meeting* (AIAA), 45–54
- 235 Guo, J., Guo, T., Zhong, M., Gao, H., Huang, B., Ding, L., et al. (2020). In-situ evaluation of terrain  
236 mechanical parameters and wheel-terrain interactions using wheel-terrain contact mechanics for wheeled  
237 planetary rovers. *Mechanism and Machine Theory* 145, 103696
- 238 Helmick, D. M., Roumeliotis, S. I., Cheng, Y., Clouse, D. S., Bajracharya, M., and Matthies, L. H. (2006).  
239 Slip-compensated path following for planetary exploration rovers. *Advanced Robotics* 20, 1257–1280
- 240 Hidalgo-Carrio, J., Babu, A., and Kirchner, F. (2014). Static forces weighted jacobian motion models for  
241 improved odometry. In *2014 IEEE/RSJ International Conference on Intelligent Robots and Systems*  
242 (IEEE), 169–175

- 243 Higa, S., Nagaoka, K., Nagatani, K., and Yoshida, K. (2015). Measurement and modeling for two-  
244 dimensional normal stress distribution of wheel on loose soil. *Journal of Terramechanics* 62, 63–73
- 245 Higa, S., Sawada, K., Teruya, K., Nagaoka, K., and Yoshida, K. (2016). Three-dimensional stress  
246 distribution of a rigid wheel on lunar regolith simulant. In *Proceedings of the 13th International*  
247 *Symposium on Artificial Intelligence, Robotics and Automation in Space, # S-9a-3*
- 248 Howard, T. M., Morfopoulos, A., Morrison, J., Kuwata, Y., Villalpando, C., Matthies, L., et al. (2012).  
249 Enabling continuous planetary rover navigation through fpga stereo and visual odometry. In *2012 IEEE*  
250 *Aerospace Conference (IEEE)*, 1–9
- 251 i Caireta, I. M. (2021). *Improving Global Localization Algorithms for Mars Rovers with Neural Networks*.  
252 Master's thesis, Aalborg University
- 253 Iagnemma, K., Kang, S., Shibly, H., and Dubowsky, S. (2004). Online terrain parameter estimation for  
254 wheeled mobile robots with application to planetary rovers. *IEEE transactions on robotics* 20, 921–927
- 255 Ishigami, G., Miwa, A., Nagatani, K., and Yoshida, K. (2007). Terramechanics-based model for steering  
256 maneuver of planetary exploration rovers on loose soil. *Journal of Field robotics* 24, 233–250
- 257 Kilic, C., Gross, J. N., Ohi, N., Watson, R., Strader, J., Swiger, T., et al. (2019). Improved planetary rover  
258 inertial navigation and wheel odometry performance through periodic use of zero-type constraints. In  
259 *2019 IEEE/RSJ International Conference on Intelligent Robots and Systems (IROS) (IEEE)*, 552–559
- 260 Kilic, C., Ohi, N., Gu, Y., and Gross, J. N. (2021). Slip-based autonomous zupt through gaussian process  
261 to improve planetary rover localization. *IEEE Robotics and Automation Letters* 6, 4782–4789
- 262 Li, Y., Ding, L., Zheng, Z., Yang, Q., Zhao, X., and Liu, G. (2018). A multi-mode real-time terrain  
263 parameter estimation method for wheeled motion control of mobile robots. *Mechanical Systems and*  
264 *Signal Processing* 104, 758–775
- 265 Lou, Q., González, F., and Kövecses, J. (2019). Kinematic modeling and state estimation of exploration  
266 rovers. *IEEE Robotics and Automation Letters* 4, 1311–1318
- 267 Maimone, M., Cheng, Y., and Matthies, L. (2007). Two years of visual odometry on the mars exploration  
268 rovers. *Journal of Field Robotics* 24, 169–186
- 269 Malinowski, M. T., Richards, A., and Woods, M. (2022). Wheel slip prediction for improved rover  
270 localization. In *AIAA SCITECH 2022 Forum*. 1080
- 271 Matijevic, J. (1997a). Characterization of martian surface deposit by the mars pathfinder rover, sojourner.  
272 *Science* 278, 237–242
- 273 Matijevic, J. (1997b). Sojourner the mars pathfinder microrover flight experiment. *Space Technology* 17,  
274 143–149
- 275 Matthies, L., Daftry, S., Tepsuporn, S., Cheng, Y., Atha, D., Swan, R. M., et al. (2022). Lunar rover  
276 localization using craters as landmarks. *arXiv preprint arXiv:2203.10073*
- 277 Nagatani, K., Ikeda, A., Ishigami, G., Yoshida, K., and Nagai, I. (2010). Development of a visual odometry  
278 system for a wheeled robot on loose soil using a telecentric camera. *Advanced Robotics* 24, 1149–1167
- 279 Ojeda, L., Cruz, D., Reina, G., and Borenstein, J. (2006). Current-based slippage detection and odometry  
280 correction for mobile robots and planetary rovers. *IEEE Transactions on robotics* 22, 366–378
- 281 Ojeda, L., Reina, G., and Borenstein, J. (2004). Experimental results from flexnav: An expert rule-based  
282 dead-reckoning system for mars rovers. In *2004 IEEE Aerospace Conference Proceedings (IEEE Cat.*  
283 *No. 04TH8720) (IEEE)*, vol. 2, 816–825
- 284 Omura, T. and Ishigami, G. (2017). Wheel slip classification method for mobile robot in sandy terrain  
285 using in-wheel sensor. *Journal of Robotics and Mechatronics* 29, 902–910
- 286 Otsu, K., Ono, M., Fuchs, T. J., Baldwin, I., and Kubota, T. (2016). Autonomous terrain classification with  
287 co-and self-training approach. *IEEE Robotics and Automation Letters* 1, 814–819



- 288 Quadrelli, M. B., Wood, L. J., Riedel, J. E., McHenry, M. C., Aung, M., Cangahuala, L. A., et al. (2015).  
289 Guidance, navigation, and control technology assessment for future planetary science missions. *Journal*  
290 *of Guidance, Control, and Dynamics* 38, 1165–1186
- 291 Reina, G., Ishigami, G., Nagatani, K., and Yoshida, K. (2010). Odometry correction using visual slip angle  
292 estimation for planetary exploration rovers. *Advanced Robotics* 24, 359–385
- 293 Reina, G., Leanza, A., and Messina, A. (2020). Terrain estimation via vehicle vibration measurement and  
294 cubature kalman filtering. *Journal of Vibration and Control* 26, 885–898
- 295 Sakai, A., Tamura, Y., and Kuroda, Y. (2009). An efficient solution to 6dof localization using unscented  
296 kalman filter for planetary rovers. In *2009 IEEE/RSJ International Conference on Intelligent Robots and*  
297 *Systems* (IEEE), 4154–4159
- 298 Sanguino, T. d. J. M. (2017). 50 years of rovers for planetary exploration: A retrospective review for future  
299 directions. *Robotics and Autonomous Systems* 94, 172–185
- 300 Strader, J., Otsu, K., and Agha-mohammadi, A.-a. (2020). Perception-aware autonomous mast motion  
301 planning for planetary exploration rovers. *Journal of Field Robotics* 37, 812–829
- 302 Vulpi, F., Milella, A., Cordes, F., Dominguez, R., and Reina, G. (2020). Deep terrain estimation for  
303 planetary rovers. In *15th International Symposium on Artificial Intelligence, Robotics and Automation in*  
304 *Space, ISAIRAS-2020*
- 305 Wan, W., Liu, Z., Di, K., Wang, B., and Zhou, J. (2014). A cross-site visual localization method for yutu  
306 rover. *The International Archives of Photogrammetry, Remote Sensing and Spatial Information Sciences*  
307 40, 279
- 308 Ward, C. C. and Iagnemma, K. (2008). A dynamic-model-based wheel slip detector for mobile robots on  
309 outdoor terrain. *IEEE Transactions on Robotics* 24, 821–831
- 310 Wong, J.-Y. and Reece, A. (1967). Prediction of rigid wheel performance based on the analysis of  
311 soil-wheel stresses: Part ii. performance of towed rigid wheels. *Journal of Terramechanics* 4, 7–25
- 312 Wu, B., WK, P. R., Ludivig, P., Chung, A. S., and Seabrook, T. (2019). Absolute localization through  
313 orbital maps and surface perspective imagery: A synthetic lunar dataset and neural network approach. In  
314 *2019 IEEE/RSJ International Conference on Intelligent Robots and Systems (IROS)* (IEEE), 3262–3267
- 315 Zhang, T., Peng, S., Jia, Y., Sun, J., Tian, H., and Yan, C. (2022a). Slip estimation model for planetary  
316 rover using gaussian process regression. *Applied Sciences* 12, 4789
- 317 Zhang, W., Lyu, S., Xue, F., Yao, C., Zhu, Z., and Jia, Z. (2022b). Predict the rover mobility over soft  
318 terrain using articulated wheeled bevameter. *IEEE Robotics and Automation Letters*